Safety & Defense 8(2) (2022)
DOI: https://doi.org/10.37105/sd.184

The Impact of Static Pressure Measurement Accuracy on Barometric Altimeter Errors

Zbigniew STANIK
zbigniew.stanik@polsl.pl
https://orcid.org/0000-0003-1965-4090
Faculty of Transport and Aviation Engineering, The Silesian University of Technology, Krasińskiego 8 Street, 40-019 Katowice, Poland

Tomasz MATYJA
tomasz.matyja@polsl.pl (Corresponding author)
https://orcid.org/0000-0001-6364-619X
Faculty of Transport and Aviation Engineering, The Silesian University of Technology, Krasińskiego 8 Street, 40-019 Katowice, Poland

Andrzej KUBIK
andrzej.kubik@polsl.pl
https://orcid.org/0000-0002-9765-6078
Faculty of Transport and Aviation Engineering, The Silesian University of Technology, Krasińskiego 8 Street, 40-019 Katowice, Poland

Received: 02 June 2022 | Revised: 18 September 2022
Accepted: 15 November 2022 | Available online: 15 December 2022

Abstract

The horizontal movement of the pressure sensor in relation to air masses may cause erroneous indications of the altimeter due to the possible measurement of the total pressure, which is the sum of the static and dynamic pressure. This problem mainly concerns devices of small dimensions equipped with barometric altimeters made in MEMS technology, performing complex movements. Small dimensions make it difficult to arrange the pressure intake slots in a way that ensures the measurement of static pressure. Examples include drones (UAH) or bike computers. The aim of the research was to develop an altitude correction formula depending on the speed of the pressure sensor relative to air, which, contrary to those found in the literature, would take into account changes in air density with altitude. The theoretical analysis of the influence of the speed of movement on the indications of the barometric altimeter was evaluated in this paper based on the standard atmosphere model. Methods of correcting errors caused by the measurement of total pressure were proposed. The effectiveness of the proposed methods was verified with simulations (Matlab). Experimental studies were also carried out, which confirmed the theoretical considerations. The experiments performed showed that the problem of correcting errors caused by incorrect measurement of static pressure is very complex. The inertia of the barometer indications plays an important role. The direction of airflow and pressure distribution on the flowing object are also important. The results presented in this paper can be used in the design of systems that improve the quality of barometric altimeter readings. This is particularly important when designing low-budget drone navigation systems and it will improve flight safety.

Keywords: barometric altimeter, error correction, external disturbance, MEMS

Safety & Defense 8(2) (2022)
DOI: https://doi.org/10.37105/sd.184

1. Introduction

Thanks to MEMS technology (Chin et al.,2011), the barometric altimeter has become an affordable and widely used device. It is currently installed in many devices: flying models, drones, bicycle computers, smartphones, etc. The barometric altimeter works much better and usually gives much more accurate altitude indications compared to the GPS system. At the same time, the barometric altimeter is sensitive to various types of disturbances and changes in weather conditions. The altimeter system converts pressure to altitude using the standard atmosphere model (ISA). If there are conditions at sea level other than standard atmospheric conditions, the indications are burdened with the so-called basic error, which is relatively easy to correct if you have up-to-date information from weather stations (Xue et al.,2017). Systems have also been developed that correct the basic error using both GPS and altimeter data (Nakanishi et al., 2012). The second type of error is due to external factors that alter the operation of the pressure sensor. Among the many sources of such disturbances is the inaccurate measurement of static pressure caused by the movement of the sensor in relation to air masses. The last type of error is the so-called barometer drift, which exhibits features of a stochastic walking process (Sabatini et al.,2013; Xue et al.,2017). The problem of correcting barometric altimeter indications is noticeable in the literature, but the available literature is not particularly rich. Attempts are made to combine information from various sensors: pressure, GPS and accelerometers and to use various methods of noisy data filtering (Popowski & Dąbrowski 2008; Seo et al.,2004; Whang et al., 2007).

This paper focuses on incorrect indications of the altimeter caused by the blowing wind and /or the movement of the instrument in relation to the ground and air, i.e., when it measures dynamic pressure. The speed of airflow near the sensor will be the result of the wind speed and the speed of the sensor. The accuracy of barometric altimeter measurements is largely dependent on the location of the pressure sampling slots. For devices with small dimensions, such as drones or bicycle computers, it is not always technically possible to measure static pressure accurately.

This paper presents theoretical considerations of the influence of dynamic pressure on the determined altitude. Methods for correcting these types of errors have been proposed and verified with simulations (Matlab). According to the authors, it is much more accurate compared to the method proposed in this paper (Xue et al.,2017), where a constant standard air density was assumed, regardless of height. Simple experiments were also carried out with the use of a pressure sensor made in MEMS technology. The aim of the experimental research was to verify the theoretical results, i.e., the proposed error correction method.

2. Theoretical background

Using the static equilibrium equation of air, the ideal gas equation (which gives rise to the formula for dry air density) and assumptions about a constant temperature gradient in the troposphere (U.S. Standard Atmosphere, 1976; Diston, 2009):

$$\frac{dp_s}{dh} = -\rho g_0 \ , \ \ \rho = \frac{p_s}{RT} \ , \ \ \frac{dT}{dh} = \lambda_0 \ \rightarrow \ \ T = T_0 + \lambda_0 (h - h_0) \tag{1}$$

the relationship between pressure and temperature can be determined:

$$\left(\frac{p_s}{p_0}\right)^{-\frac{R\lambda_0}{g_0}} = \frac{T}{T_0} \tag{2}$$

where: p_s – static pressure of the air column, h - geopotential height, ρ – air density, R – gas constant of dry air, T – air temperature (°K), λ_0 – temperature gradient in the troposphere, h_0 – reference altitude (e.g., sea level).

Then equation (2) on the basis of the dependence of temperature on altitude (1) can be transformed into the generally known formula for the pressure height, which is used in the barometric altimeter:

$$h = h_0 + \frac{T_0}{\lambda_0}\left[\left(\frac{p}{p_0}\right)^{-\frac{R\lambda_0}{g_0}} - 1\right] \tag{3}$$

In further consideration, in order to simplify the notation without losing generality, it was assumed $h_0 = 0$.

If the pressure sensor moves horizontally in relation to the air masses at speed V, the instrument measures the total pressure, which is the sum of the static and dynamic pressures:

Safety & Defense 8(2) (2022)
DOI: https://doi.org/10.37105/sd.184

$$p = p_s + \alpha\frac{1}{2}\rho V^2 \quad \rightarrow \quad p = p_s\left(1 + \alpha\frac{V^2}{2RT}\right) \tag{4}$$

In formula (4), the factor $\alpha \leq 1$ allows us to take into account the fact that the overpressure at the pressure sampling point may be lower than the maximum dynamic pressure at the point of stagnation. Theoretically, the pressure sampling point may also be located in the negative pressure zone, and the coefficient α may have negative values. The pressure p in formula (4) is the pressure measured by the instrument. After substituting (4) to (2) and transforming, the following formula is obtained:

$$\left(\frac{p}{p_0}\right)^{-\frac{R\lambda_0}{g_0}} = \left(1 + \alpha\frac{V^2}{2RT}\right)^{-\frac{R\lambda_0}{g_0}}\frac{T}{T_0} \tag{5}$$

After entering dimensionless parameters:

$$\left(\frac{p}{p_0}\right) = p_* \,, \quad \left(\frac{T}{T_0}\right) = T_* \,, \quad m = \frac{R\lambda_0}{g_0} \,, \quad V_* = \alpha\frac{V^2}{2RT_0} \ll 1 \tag{6}$$

formula (5) can be written as:

$$p_*^{-m} = \left(1 + \frac{V_*}{T_*}\right)^{-m} T_* \tag{7}$$

The dimensionless temperature T_* can be determined directly from formula (7) only by numerical methods. Alternatively, the temperature T_* can be estimated from approximate formulas. To do this, the expression needs to be expanded into a binomial series:

$$\left(1 + \frac{V_*}{T_*}\right)^{-m} \approx 1 - m\frac{V_*}{T_*} + \frac{1}{2}m(m+1)\left(\frac{V_*}{T_*}\right)^2 - \cdots \tag{8}$$

It is not hard to find out that dimensionless speed V_* is much smaller than unity (in the range of real values, e.g., to $60m/s$). Therefore, the series convergence condition is fulfilled $\left|\frac{V_*}{T_*}\right| \leq 1$.

If only the first three terms of the series are taken into account, after substituting (8) to (5), a quadratic equation can be obtained due to T_*:

$$T_*^2 - (mV_* + p_*^{-m})T_* + \frac{1}{2}m(m+1)V_*^2 = 0 \tag{9}$$

whose solutions are:

$$T_* = \frac{1}{2}(mV_* + p_*^{-m}) \pm \frac{1}{2}\sqrt{(mV_* + p_*^{-m})^2 - 2\left(1 + \frac{1}{m}\right)(mV_*)^2} \tag{10}$$

After the dimensions are restored, the first factor in (10) will take the form:

$$mV_* + p_*^{-m} = \frac{R\lambda_0}{g_0}\alpha\frac{V^2}{2RT_0} + \left(\frac{p}{p_0}\right)^{-\left(\frac{R\lambda_0}{g_0}\right)} = \frac{\lambda_0}{T_0}\alpha\frac{V^2}{2g_0} + \left(\frac{p}{p_0}\right)^{-\left(\frac{R\lambda_0}{g_0}\right)} \tag{11}$$

Safety & Defense 8(2) (2022)
DOI: https://doi.org/10.37105/sd.184

second:

$$2\left(1+\frac{1}{m}\right)(mV_*)^2 = 2\left(1+\frac{g_0}{R\lambda_0}\right)\left(\frac{\lambda_0}{T_0}\alpha\frac{V^2}{2g_0}\right)^2 \tag{12}$$

The concept of speed height can be introduced h_{V0} (analogous to the Bernoulli equation): and the measured pressure p can be replaced by the measured height h_m:

$$h_{V0} = \alpha\frac{V^2}{2g_0}, \qquad \left(\frac{p}{p_0}\right)^{-\left(\frac{R\lambda_0}{g_0}\right)} = \frac{\lambda_0}{T_0}h_m + 1 \tag{13}$$

Based on (10), taking into account (11-13) and dependence $T_* = 1 + \frac{\lambda_0}{T_0}h$, an approximate formula can be obtained for the real (corrected) height:

$$h \approx \frac{1}{2}\left(h_{V0} + h_m + \frac{T_0}{\lambda_0}\right) \pm \frac{1}{2}\sqrt{\left(h_{V0} + h_m + \frac{T_0}{\lambda_0}\right)^2 - 2\left(1+\frac{g_0}{R\lambda_0}\right)h_{V0}^2} - \frac{T_0}{\lambda_0} \tag{14}$$

In order to determine which of the solutions (14) makes physical sense, the following reasoning can be made. When $V \to 0$ then $h \to h$, that is:

$$\lim_{V\to 0} h = \frac{1}{2}\left(h_m + \frac{T_0}{\lambda_0}\right) \pm \frac{1}{2}\left|h_m + \frac{T_0}{\lambda_0}\right| - \frac{T_0}{\lambda_0} \to h_m \tag{15}$$

Since $\frac{T_0}{\lambda_0} = -44331m$ is the expression $h_m + \frac{T_0}{\lambda_0}$, for tropospheric heights $h_m \leq 11000m$ will always be negative. This means that there is a physical sense to the negative solution:

$$h \approx \frac{1}{2}\left(h_{V0} + h_m + \frac{T_0}{\lambda_0}\right) - \frac{1}{2}\sqrt{\left(h_{V0} + h_m + \frac{T_0}{\lambda_0}\right)^2 - 2\left(1+\frac{g_0}{R\lambda_0}\right)h_{V0}^2} - \frac{T_0}{\lambda_0} \tag{16}$$

The error between the measured height and the real height can be estimated by using the formula:

$$\Delta h = h - h_m \tag{17}$$

Further transformations equation (16):

$$h \approx \left(h_{V0} + h_m + \frac{T_0}{\lambda_0}\right)\left(\frac{1}{2} + \frac{1}{2}\sqrt{1 - \frac{2\left(1+\frac{g_0}{R\lambda_0}\right)h_{V0}^2}{\left(h_{V0} + h_m + \frac{T_0}{\lambda_0}\right)^2}}\right) - \frac{T_0}{\lambda_0} \tag{18}$$

and the observation that the second factor under the root is much smaller than one allow us to propose another approximation of the formula to the real height:

$$h \approx h_m + h_{V0} - \frac{1}{2}\frac{\left(1+\frac{g_0}{R\lambda_0}\right)h_{V0}^2}{\left(h_{V0} + h_m + \frac{T_0}{\lambda_0}\right)} \tag{19}$$

Safety & Defense 8(2) (2022)
DOI: https://doi.org/10.37105/sd.184

Or even further:

$$h \approx h_m + h_{V0} \tag{20}$$

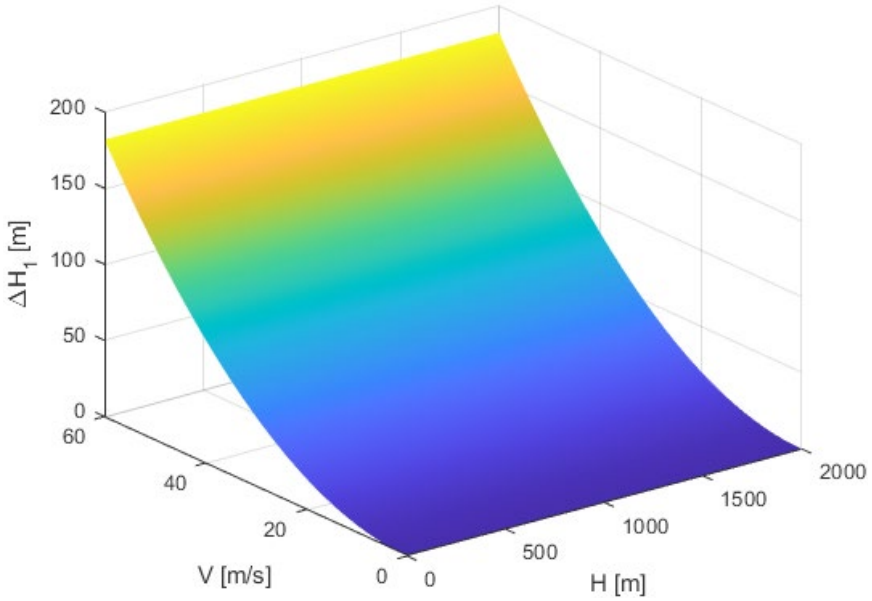

Figure 1. The altitude error calculated from equation (16)
Authors' own work.

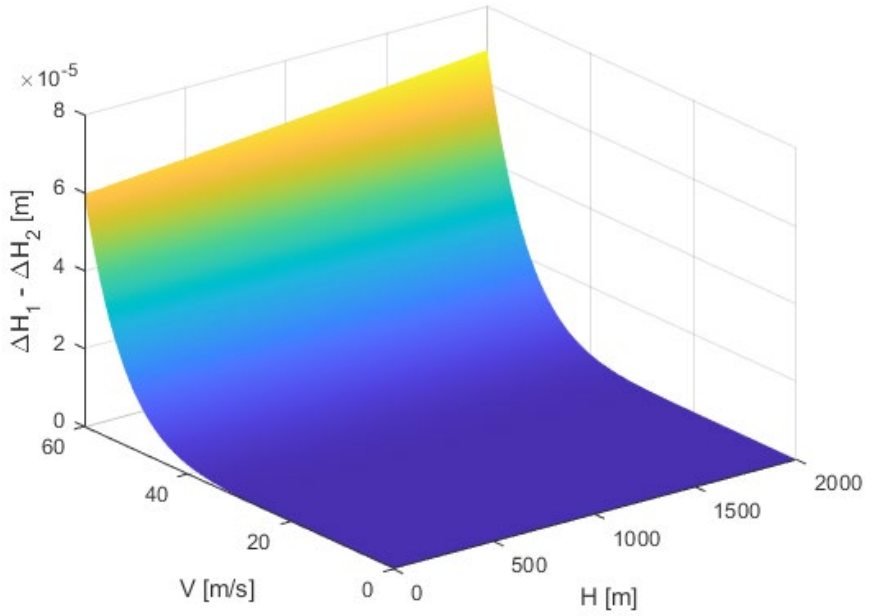

Figure 2. The difference of altitude errors calculated from equation (16) and (19)
Authors' own work.

Fig. 1 shows the error of altitude determined by the barometric altimeter for different values of speed and altitude ($\alpha = 1$ was assumed). The error calculated from the approximate formulas (16) and (17) was marked as ΔH_1. It can be seen that this error grows squarely with speed but practically does not depend on the height itself. The errors calculated from formulas (19) and (20)

Safety & Defense 8(2) (2022)
DOI: https://doi.org/10.37105/sd.184

were marked as ΔH_2 and ΔH_3, respectively. Fig. 2 shows the difference between the errors $\Delta H_1 - \Delta H_2$ and in Fig. 3 the difference between the errors $\Delta H_1 - \Delta H_3$.

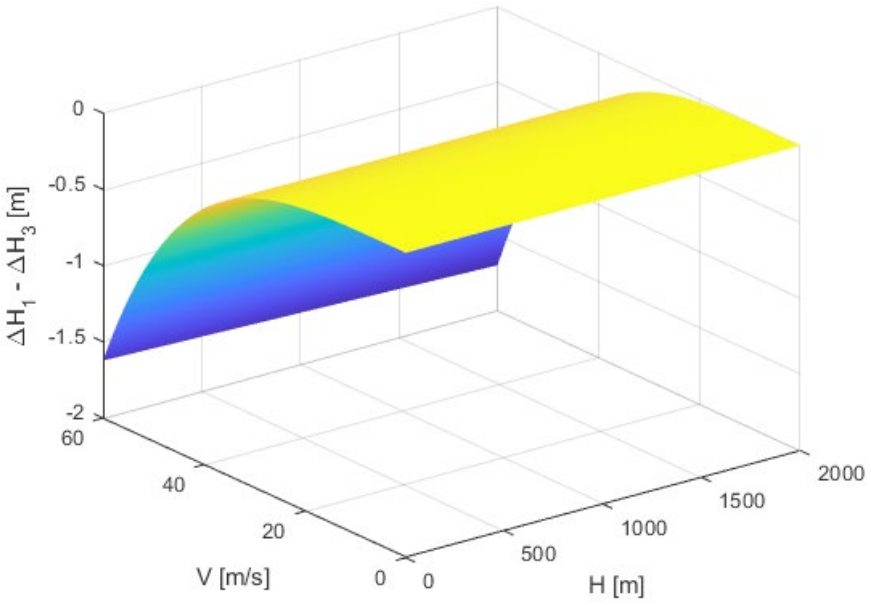

Figure 3. The difference of altitude errors calculated from equation (16) and (20)
Authors' own work.

It can be seen that the results obtained from formulas (19) and (16) are practically identical. On the other hand, in the case of correcting the height using the formula (20), the error of 1% should be overestimated. At the same time, the advantage of formula (20) is due to its simplicity and independence from the current height.

3. Materials, Methods and Experiment Course

The study used a barometric pressure gauge made in MEMS technology by Bosch - the BMP280 model connected to the ATMEGA328P-PU microcontroller using communication via the I2C bus. Figures 4a and 4b show the transducer itself and the transducer built into the bicycle computer housing during the measurements.

a) b)

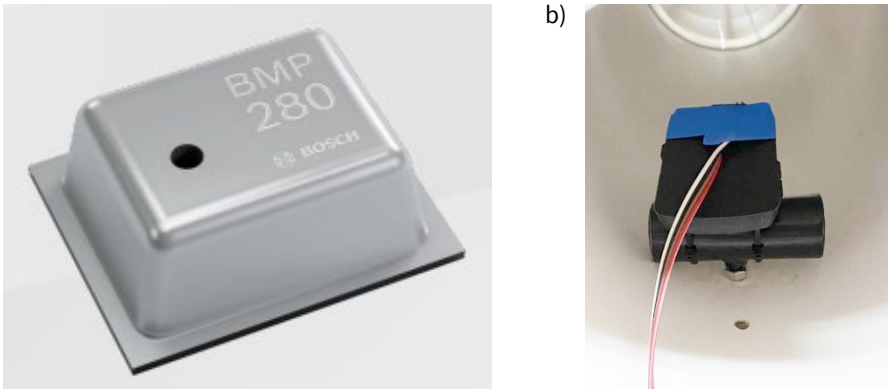

Figure 4. Pressure and temperature transducer (a) used in the tests (*https://www.bosch-sensortec.com/bst-bmp280-ds001.pdf*, 2022) and sensor mounted on the actual housing of the bicycle computer (b)
Authors' own work.

Safety & Defense 8(2) (2022)
DOI: https://doi.org/10.37105/sd.184

The experiment used a 230VAC duct fan with a speed regulator (potentiometer adjustment), which was built into a part of the ventilation pipe (Fig. 5.)

Figure 5. Measuring in the 'wind tunnel'
Authors' own work.

Figure 6. Anemometer used during the tests
Authors' own work.

The rotational speed of the fan was regulated by a potentiometer. The flow velocity in the prepared "wind tunnel" was measured with a Chauvin-Anoux anemometer - model C.A. 1227, which is shown in Fig. 6.

Additionally, the rotational speed of the fan was also measured using a laser sensor module and a laser receiver module with a wavelength of 650nm, mounted on both sides of the fan. Such a location allows for each rotation of one fan blade to be counted. The digital signal from the receiver module is sent to the ATMEGA328P-PU microcontroller. The position of the modules is shown in Figures 4a and 4b.

Then, all data from the I2C bus and digital signals of the fan rotational speed were processed by the ATMEGA328P-PU microcontroller and then sent via the serial bus to a PC.

a) b)

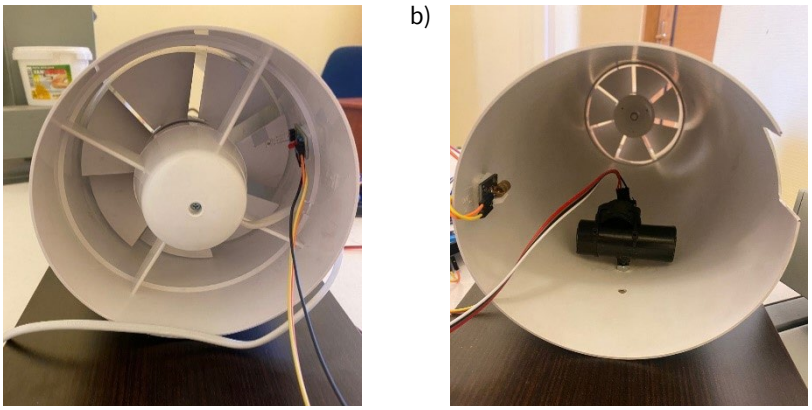

Figure 7. View of the location of the laser sensor module (b) and the receiver module (a) in the measurement tunnel
Authors' own work.

Two simple experiments were performed. The first, a static experiment, which consisted of setting the potentiometer, regulating the fan speed in a specific position, and measuring the flow speed with an anemometer. Then a plate with a pressure transducer perpendicular to the flow direction was placed in the air stream. After the readings stabilized, the total pressure value measured by the sensor was recorded.

Safety & Defense 8(2) (2022)
DOI: https://doi.org/10.37105/sd.184

The second experiment consisted of the dynamic change of the potentiometer settings and the continuous reading of the pressure value. The rotational speed of the windmill was also recorded and converted to the flow velocity. Previously, the rotational speed of the fan was calibrated with the flow velocity measured by the anemometer to make such a conversion possible.

4. Results analysis and discussion

The results of the static experiment are shown in Fig. 8. The fan-generated an airflow speed of 1.7m/s, 4m/s and 6m/s, as indicated by the anemometer. The recorded total pressure was converted to the altitude, and the error of indication caused by the airflow was calculated. The diagram shows the maximum value of the correction (factor $\alpha = 1$), which can be made using the formula (20). A correlation of the correction and the error is visible, which means that after applying the correction, the erroneous indications of the altimeter will be reduced almost to zero. It should be noted that in Fig. 8 (later also in Fig. 11), the value of the height correction is given with a minus sign in order to better visualize the correlation between the error and the correction.

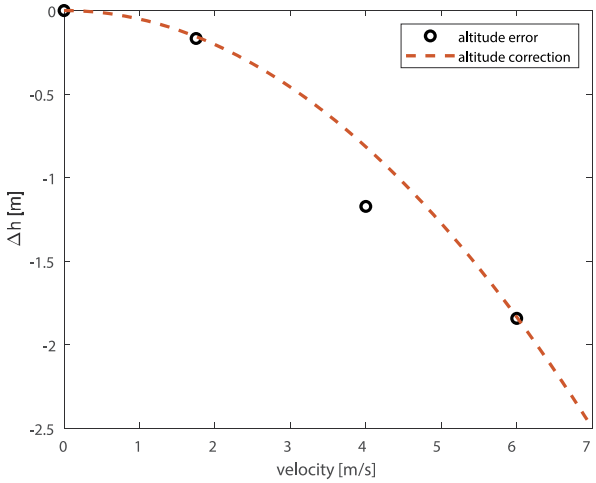

Figure 8. The altimeter error and its correction using velocity height (Eq.20)
Authors' own work.

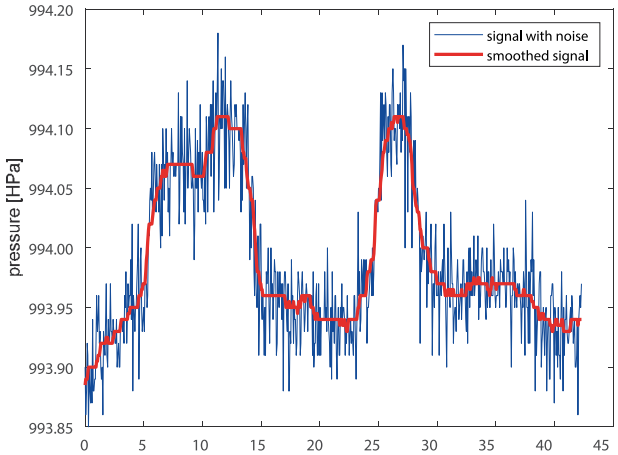

Figure 9. Pressure signals measured and smoothed
Authors' own work.

In the second experiment, the total pressure signal and the air velocity measured with a frequency of 17.24 Hz were obtained. The airflow speed resulted directly from the measured rotational speed of the windmill of the duct fan. Due to the significant noise, these signals were smoothed with a moving median filter (Fig. 9 and Fig. 10). On the basis of the smoothed pressure signal, the

Safety & Defense 8(2) (2022)
DOI: https://doi.org/10.37105/sd.184

dynamic changes of the altimeter indications error were calculated. On the other hand, on the basis of the smoothed flow velocity signal, dynamic changes in the correction value were determined. The results are shown in Fig. 11. In this case, the agreement of error and correction is much worse than in the static experiment. The barometer clearly reacts with a certain delay to changes in dynamic pressure. At the same time, the changes take place in a relatively short time.

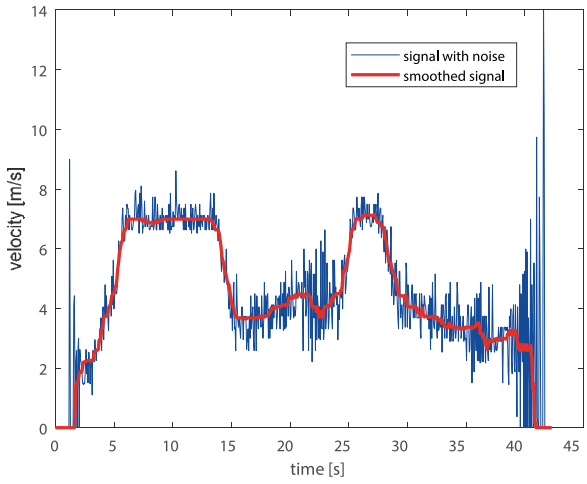

Figure 10. Air velocity signals measured and smoothed
Authors' own work.

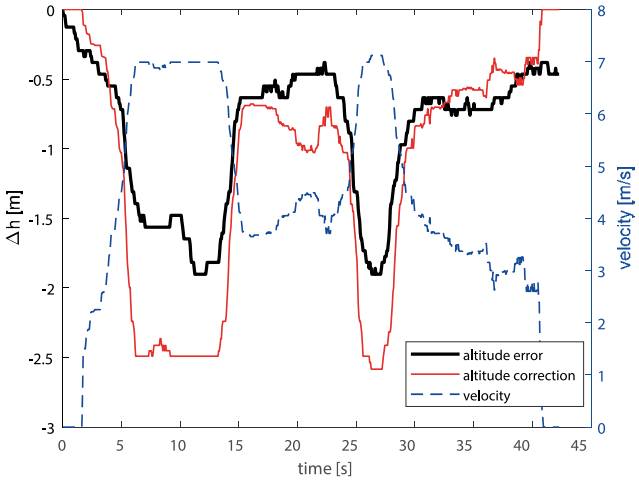

Figure 11. Dynamic changes of the altimeter error and its corrections based on the flow velocity
Authors' own work.

5. Conclusions

The formula for the dependence of temperature on the pressure in the standard atmosphere derived in this work, taking into account the influence of the sensor velocity and the related dynamic pressure, is highly non-linear and can only be solved numerically. However, as shown, approximate solutions can be used. One of them has a very simple mathematical form and is quite accurate at the same time. The barometric altimeter error can be effectively corrected by adding to the measured value a correction altitude which has a very simple physical interpretation. This is the so-called speed height, by analogy to the nomenclature used in the description of the Bernoulli equation.

The simple experiments carried out confirm the possibility of an effective correction of the altitude error caused by the air movement in relation to the sensor. This is the case where the pressure sampling point can be assumed to be at or near the velocity

Safety & Defense 8(2) (2022)
DOI: https://doi.org/10.37105/sd.184

stagnation point. An effective correction requires the determination of the pressure distribution coefficient in the flow around the body (device) in which the sensor was mounted. At the same time, studies have shown that there is a large influence of the sensor inertia on the pressure measurement results.

It is possible to conduct more precise tests at higher flow velocities and in more stable flow conditions in a professional wind tunnel. Research in the tunnel will allow us to gain knowledge about the flow pressure distribution in selected conditions of movement of the device equipped with a pressure sensor. In conjunction with the method proposed in this work, it is possible to develop a system for correcting altitude errors caused by the relative movement of the sensor and the air.

Declaration of interest –The authors declare that they have no known competing financial interests or personal relationships that could have appeared to influence the work reported in this article.

References

1. Diston D.J. (2009). *Computational Modelling and Simulation of Aircraft and the Environment: Platform Kinematics and Synthetic Environment*. *Volume 1*. John Wiley & Sons, Ltd.
2. Lin C.E., Huang W.-C., & Nien C.-C. (2011). MEMS-Based Air Data Unit with Real Time Correction for UAV Terrain Avoidance. *Journal of Aeronautics, Astronautics and Aviation, Series A, Vol*.43, No.2 pp.103 – 110. https://www.researchgate.net/publication/224358008.
3. Sabatini A. M., & Genovese V. (2013). A Stochastic Approach to Noise Modeling for Barometric Altimeters, *Sensors*, *Vol.*13, No.11, pp.15692-15707. DOI: 10.3390/s131115692
4. *Pressure and temperature sensor BMP280*. Available online: https://www.bosch-sensortec.com/media/boschsensortec/downloads/datasheets/bst-bmp280-ds001.pdf (accessed on 30 January 2022).
5. *U.S. Standard Atmosphere* (1976). U.S. Government Printing Office, Washington, D.C.
6. Nakanishi, H., Kanata S., & Sawaragi T. (2012). GPS-INS BARO hybrid navigation system taking into account ground effect for autonomous unmanned helicopter, *IEEE International Symposium on Safety, Security, and Rescue Robotics*, pp. 1-6. DOI: 10.1109/SSRR.2012.6523885.
7. Popowski S.,& Dąbrowski W. (2008). An Integrated Measurement of Altitude and Vertical Speed for UAV. *Transport and Engineering. Transport. Aviation Transport. Scientific Proceedings of Riga Technical University*, Series 6, N27. pp.197-205. Riga, RTU.
8. Seo J., Lee J. G., & Park C.G. (2004). Bias suppression of GPS measurement in inertial navigation system vertical channel, *Position Location and Navigation Symposium*, pp. 143-147. DOI: 10.1109/PLANS.2004.1308986.
9. Whang I-H., & Ra W. S. (2007). Barometer error identification filter design using sigma point hypotheses, *International Conference on Control, Automation and Systems*, pp. 1410-1415. DOI: 10.1109/ICCAS.2007.4406559.
10. Bao X., Xiong Z., Sheng S., Dai Y., Bao S., & Liu J. (2017). Barometer Measurement Error Modeling and Correction for UAH Altitude Tracking. *29th Chinese Control and Decision Conference (CCDC)*. pp.3166-3171. DOI:10.1109/CCDC.2017.7979052